MSDE

PAPER

View Article Online
View Journal

Cite this: DOI: 10.1039/d2me00004k

An energetics assessment of benzo[*a*]tetracene and benzo[*a*]pyrene as triplet–triplet annihilation emitters†

Xiaopeng Wang *[a] and Noa Marom [bcd]

Received 13th January 2022,
Accepted 13th April 2022

DOI: 10.1039/d2me00004k

rsc.li/molecular-engineering

Optical upconversion (UC) of low energy photons into high energy photons enables solar cells to harvest photons with energies below the band gap of the absorber, reducing the transmission loss. UC based on triplet–triplet annihilation (TTA) in organic chromophores can upconvert photons from sunlight, albeit with low conversion efficiency. We utilize three energy-based criteria to assess the UC potential of TTA emitters in terms of the quantum yield (QY) and the anti-Stokes shift. The energy loss in the singlet pathway of an emitter encounter complex, where a high energy photon is emitted, determines whether a chromophore may undergo TTA. The energy loss in the triplet pathway, which is the main competing process, impacts the TTA QY. The energy difference between the lowest singlet and triplet excitation states in TTA emitters sets an upper bound for the anti-Stokes shift of TTA-UC. Using the energetic criteria evaluated by time-dependent density functional theory (TDDFT) calculations, we find that benzo[*a*]tetracene, benzo[*a*]pyrene, and their derivatives are promising TTA emitters. The energetics assessment and computer simulations could be used to efficiently discover and design more candidate high-performance TTA emitters.

Design, System, Application

Triplet–triplet annihilation (TTA) is the conversion of two low-energy triplet excitons into one high-energy singlet exciton in organic molecules. Up-conversion (UC) by TTA has the potential to increase the efficiency of solar cells by harvesting photons with energies below the gap of the absorber. Currently, known TTA emitters are rare, the TTA quantum yield (QY) is low, and the anti-Stokes shift of TTA-UC is usually small, hindering the practical device application of TTA-UC. We analyze how the energies of the excited states involved impact the TTA-UC performance in terms of the TTA QY and the anti-Stokes shift. Based on this analysis, we propose energetic criteria to assess prospective TTA emitters. These criteria may aid the computational discovery and design of new TTA emitters, using first principles quantum mechanical simulations based on time dependent density functional theory (TDDFT). Utilizing this strategy, new chemical families and chemical functionalization may be explored to optimize the performance of TTA emitters. The manuscript may potentially influence future directions in the search and design of new TTA emitters, which would lead to advancements in solar cell efficiency.

1 Introduction

Photovoltaic devices such as solar cells suffer from limited efficiencies due to spectral losses.[1] Photons with energy below the band gap of the absorber cannot be harvested. Surplus energy from photons with energy above this threshold is converted into heat. These transmission and thermalization losses restrain the conversion efficiency of solar energy.[2,3] The former loss of the sub-band-gap light may be mitigated by optical upconversion (UC) of two low energy photons into one high energy photon.[3–5] Among the UC mechanisms, UC based on sensitized triplet–triplet annihilation (TTA)[2,5–10] in organics is particularly appealing because it upconverts incoherent light at low intensities, such as sunlight.[4,7]

The TTA-UC is accomplished in mixtures of sensitizer and emitter chromophores, as illustrated in Fig. 1. A sensitizer absorbs an incident photon and subsequently converts the lowest singlet state, $S_1(S)$, into a lowest triplet state, $T_1(S)$, *via* inter-system crossing (ISC). Next, triplet excitons are transferred from the sensitizer to the emitter, $T_1(E)$, through a Dexter process,[8,11–13] triplet–triplet energy transfer (TTET). Two triplet emitters then interact and undergo TTA, producing one emitter molecule in the lowest singlet excited state, $S_1(E)$, and leaving the other molecule in its ground

[a] *Qingdao Institute for Theoretical and Computational Sciences, Institute of Frontier and Interdisciplinary Science, Shandong University, Qingdao, Shandong 266237, P. R. China. E-mail: xiaopengwang@sdu.edu.cn*
[b] *Department of Materials Science and Engineering, Carnegie Mellon University, Pittsburgh, PA 15213, USA*
[c] *Department of Physics, Carnegie Mellon University, Pittsburgh, PA 15213, USA*
[d] *Department of Chemistry, Carnegie Mellon University, Pittsburgh, PA 15213, USA*

† Electronic supplementary information (ESI) available: The excitation energies of known emitters, visualization of frontier orbitals for phenanthrene, and spectral composition of T_2 states for BA, BT, and BP. See DOI: https://doi.org/10.1039/d2me00004k

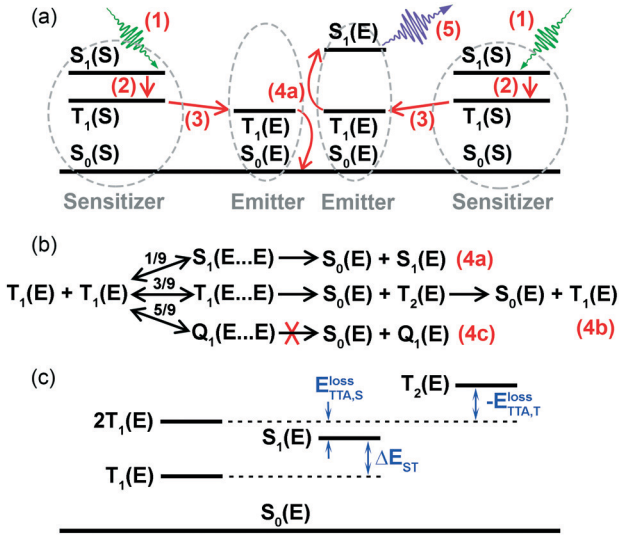

Fig. 1 (a) Schematic of the five processes involved in TTA-UC: (1) absorption, (2) ISC, (3) TTET, (4a) TTA, and (5) fluorescence. The *S* and *E* in the parentheses indicate the sensitizer and emitter. The incident and upconverted photons are shown in green and purple. (b) The (4a) singlet, (4b) triplet, and (4c) quintet pathways of an emitter triplet encounter complex with their spin-statistical probabilities. (c) Excitation energies of an optimal emitter.

state, $S_0(E)$. Finally, an upconverted photon is emitted when an emitter singlet decays radiatively. The quantum yield (QY) of TTA would be 50% if two low energy triplets were upconverted into one high energy singlet.[14] However, there are two other possible pathways[15–17] of an emitter triplet encounter complex,[18] as shown in Fig. 1(b). In the triplet pathway, an emitter encounter complex converts into one molecule in a highly excited triplet state, usually the second triplet excited state, $T_2(E)$, and the other molecule in its ground state. The $T_2(E)$ state may further decay back into a $T_1(E)$ state without producing an upconverted $S_1(E)$ state in this pathway. The quintet pathway is usually inaccessible because the product of an emitter in its quintet state, $Q_1(E)$, is too high in energy. Considering only the singlet pathway and the competing triplet pathway in Fig. 1(b), the overall statistical limit of TTA QY is only 20%.[14,15]

The excitation energies of the sensitizer and emitter pair must meet several requirements, as illustrated in Fig. 1(a). The lowest singlet and triplet excitation energies of the sensitizer should be nested between those of the emitter, $T_1(S) > T_1(E)$ and $S_1(S) < S_1(E)$. The former enables an energetically downhill TTET from the sensitizer to the emitter. The latter is required by the anti-Stokes fluorescence of TTA-UC, which corresponds to the energy difference between the incident and the upconverted photons. The larger the anti-Stokes shift, the wider spectral range of sub-band-gap photons can be upconverted. In particular, the performance of TTA emitters is determined by the energy losses in the singlet and triplet pathways:[14,19–23]

$$E_{\mathrm{TTA},S}^{\mathrm{loss}} = 2T_1(E) - S_1(E) \quad (1)$$

$$E_{\mathrm{TTA},T}^{\mathrm{loss}} = 2T_1(E) - T_2(E) \quad (2)$$

We previously evaluated the $E_{\mathrm{TTA},S}^{\mathrm{loss}}$ and $E_{\mathrm{TTA},T}^{\mathrm{loss}}$ energies for a set of 59 molecules including 16 experimentally observed TTA emitters.[14] Experimentally observed emitters exhibit a positive $E_{\mathrm{TTA},S}^{\mathrm{loss}}$ such that the TTA singlet pathway is exothermic. In comparison, $E_{\mathrm{TTA},S}^{\mathrm{loss}}$ is verified to be negative in molecules that undergo singlet fission (SF), the reverse process of TTA.[14,24,25] Ideally, the TTA QY may approach 50% if the triplet pathway is closed due to a negative energy release, $E_{\mathrm{TTA},T}^{\mathrm{loss}}$. For most known emitters, the energy release in the triplet pathway is however positive and larger than the energy release in the singlet pathway, leading to an energetically more favorable competing triplet pathway.[14] This explains why there are so few known TTA emitters and why the experimentally observed QY is often only a few percent,[6,15] much smaller than the 20% spin statistical limit. This hinders the application of TTA-UC. The $E_{\mathrm{TTA},S}^{\mathrm{loss}}$ and $E_{\mathrm{TTA},T}^{\mathrm{loss}}$ are thus the main performance parameters to be evaluated for computational discovery of new emitters and optimization of their performance *via* chemical functionalization.[14,19–22] For example, based on its $E_{\mathrm{TTA},S}^{\mathrm{loss}}$, phenyl-substituted benzothiadiazole has been computationally predicted to be a potential emitter, which was then validated by experiments.[19] Quantum chemical calculations and machine learning models have been applied in high-throughput screening of molecular databases in search of candidate emitters with favorable energy level alignment.[23]

In addition to a positive $E_{\mathrm{TTA},S}^{\mathrm{loss}}$ and a $E_{\mathrm{TTA},T}^{\mathrm{loss}}$ as negative as possible, a new energy criterion is utilized in this work to assess TTA emitters. Achieving a high QY with a large anti-Stokes shift is critical to TTA-UC applications, but remains a great challenge. For example, the highest anti-Stokes shift obtained with TTA-UC to date is only about 1.10 eV.[26,27] As shown in Fig. 1(a), the anti-Stokes shift between the incident and upconverted photons is approximately equal to the energy difference between singlet states of the sensitizer and emitter, $S_1(S)$ and $S_1(E)$. Thus, the anti-Stokes shift is increased by minimizing the energy difference among $S_1(S)$, $T_1(S)$, and $T_1(E)$ and maximizing the energy difference between $S_1(E)$ and $T_1(E)$:

$$\Delta E_{ST} = S_1(E) - T_1(E) \quad (3)$$

The minimization may be achieved by utilizing thermally activated delayed fluorescence (TADF) chromophores with similar singlet and triplet energies as sensitizers, $S_1(S) \approx T_1(S)$,[28–32] and simultaneously an appropriate choice of sensitizer and emitter pair with similar triplet energies, $T_1(S) \approx T_1(E)$.[14] The maximization of ΔE_{ST} may be employed as an additional criterion to assess the ability of emitters to upconvert photons.

The three energy criteria correspond to two requirements of relative energies of different emitter excitation states. Fig. 1(c) shows the excitation energies of an ideal TTA

emitter. First, the lowest singlet state $S_1(E)$ should be lower than, but very close to double of the lowest triplet state, $2T_1(E)$, such that the positive energy loss $E^{\text{loss}}_{\text{TTA},S}$ is minimized and ΔE_{ST} is maximized together. Notably, there is an upper bound of the anti-Stokes shift. This is because ΔE_{ST} is smaller than $T_1(E)$, as shown in Fig. 1(c), and $T_1(E)$ has a lower energy than the incident sub-band-gap photon. A large $T_1(E)$ is necessary to increase the anti-Stokes shift but narrows the incident photon energy range that can be converted. Second, $T_2(E)$ is expected to be larger than $2T_1(E)$, but is usually even lower than $S_1(E)$ in known TTA emitters.[14] Fortunately, these energy criteria are independent of each other and may be employed in the screening of TTA emitters for the rational design of upconversion materials.[23]

TTA emitters are organic chromophores, usually polycyclic aromatic hydrocarbons (PAHs).[4,6,8,13,15,17,33] For example, most of known emitters are anthracene, pyrene, perylene, and their derivatives. To discover efficient emitters, we study excitation energies of some small PAHs consisting of 3, 4, or 5 conjugated atomic rings using time-dependent density functional theory (TDDFT).[34,35] Three criteria are employed in the energetics assessment. The $E^{\text{loss}}_{\text{TTA},S}$ determines whether the chromophore may undergo TTA or SF. The $E^{\text{loss}}_{\text{TTA},T}$ and ΔE_{ST} are utilized to evaluate their UC performance through the TTA QY and anti-Stokes shift. We computationally identify benzo[*a*]tetracene (BT) and benzo[*a*]pyrene (BPy) as promising TTA emitters. Chemical modification may further improve their performance. Incorporating computer simulations as a part of the materials development pipeline can help achieve optimal performance in TTA-UC.

2 Methods

All calculations were conducted using version 4.2.0 of the ORCA code.[36] Geometries were optimized using a pairwise dispersion correction with the Becke–Johnson damping[37] and tight SCF convergence criteria. The B3LYP functional[38] and def2-TZVP basis sets were utilized in geometry optimization and TDDFT calculations. Vertical excitation energies are calculated with the optimized ground state geometries because the optical absorption corresponds to vertical excitations, based on the Franck–Condon principle. The effect of geometry relaxation on excited states is usually neglected in TDDFT screening of TTA emitters, owing to the high computational cost of excited state Hessian evaluations.[33] The energy exchange between identical molecules may be a nearly adiabatic process.[13]

TDDFT is a formally exact theory, but its predictive power strongly depends on the choice of approximation for the exchange–correlation (xc) functional. Commonly used functionals typically perform well for valence excited states, such as those of known TTA emitters. However, problems may arise for charge-transfer (CT) excited states, doubly excited states, valence states of extended π-systems, and Rydberg states.[39] The CT excitation energies may be underestimated, in particular when using semi-local xc functionals, because the self-interaction error (SIE) in DFT causes severe underestimation of the ground state HOMO–LUMO gaps and destabilizes localized molecular orbitals. This issue propagates to the TDDFT excitation energies.[40–42] In global hybrid functionals, the effect of SIE is mitigated by mixing a fraction of exact (Fock) exchange with the semi-local exchange and correlation. To correct CT excitation energies, the percentage of Fock exchange in global hybrid functionals needs to be very large, such that the results approximate Hartree Fock theory, which is detrimental to the overall accuracy.[42] Range-separated hybrid functionals improve the accuracy of CT excitations and the overall spectrum[42] by splitting the Coulomb interaction into a short-range and a long-range component and including a high fraction of exact exchange in the long range. Recently, range-separated double hybrid (RSDH) functionals have achieved further improvement by including perturbative second-order correlation (PT2) in addition to exact exchange.[43,44] The RSDH functionals perform very well for CT excitations.[45] For valence excited states of extended π-systems and Rydberg states, the failure of standard xc functionals is attributed to the wrong long-range behavior that decays faster than $1\ r^{-1}$. Asymptotically corrected functionals, which contain 100% exact exchange in the long range, thus substantially improve excitation energies of valence states of extended π-systems and Rydberg states.[39,41,46] States with substantial double excitation character are beyond the reach of linear response TDDFT because there are only singly excited states in the linear response formalism.[39,47,48] This may be solved by allowing the xc kernel to be frequency/energy dependent because the xc kernel is strongly frequency-dependent close to a double excitation.[39,47,48]

Several studies have benchmarked the performance of TDDFT with different exchange–correlation functionals.[49–51] Some have focused specifically on TTA sensitizers and emitters.[33,52] Of the hybrid generalized gradient approximation (GGA) functionals, hybrid meta-GGA functionals, and range-separated hybrid functionals, the B3LYP functional has been shown to perform consistently well for singlet and triplet excitation energies of representative sensitizers and emitters.[33] A redshift mean average error of 0.09 and 0.11 eV for S_1 and T_1 was obtained with the B3LYP functional, which was smaller than the blueshift of 0.24 and 0.12 eV for S_1 and T_1 obtained with the range-separated CAM-B3LYP[53] functional.[33] The Tamm–Dancoff approximation did not improve the description of singlet and triplet energies of sensitizer/emitter pairs.[33] The accuracy of TDDFT@B3LYP excitation energies has been verified for other systems by comparison to high level multi-reference methods and experiments.[54,55] In a TDDFT study of graphene quantum dots, which also considered the solvent effect,[55] the B3LYP functional outperformed other functionals, such as the CAM-B3LYP[53] functional and the LC-ωPBE long-range corrected range-separated hybrid functional.[56]

An appropriate choice of the xc functional is crucial in order to accurately evaluate the TTA performance metrics of chromophores based on the energetic criteria proposed here.

Thus, we begin by assessing the performance of TDDFT@B3LYP for 15 known TTA emitters, denoted as **1** to **15** in Fig. 2.

Fig. 2 shows a comparison of TDDFT@B3LYP S_1 and T_1 to experimental data.[17,20,33,57–78] Notably, the experiments were conducted at finite temperature and in different solvents, whose effects were not taken into account in our calculations. Overall, the TDDFT results are in very good agreement with experiments across different chemical families. We note that both the systematic error of the B3LYP functional and solvent effects in experiments redshift the excitation energies and may contribute to the agreement in Fig. 2. It has been shown that the redshift due to the solvent effect is negligible in comparison to the influence of the choice of functional.[79,80] For example, the difference in the absorption energies of oligopolyfurans observed in the polar solvent, ethanol, and in the non-polar solvent, benzene, was within 0.06 eV.[81]

One outlier in Fig. 2 is α-sexithiophene (α-6T, **15**), whose S_1 is underestimated by up to 0.5 eV. The S_1 energy of α-6T obtained here agrees with another TDDFT@B3LYP study.[80] This underestimation is also present[14] when using the alternative approach of many-body perturbation theory (MBPT) within the GW approximation and the Bethe–Salpeter equation (BSE).[82–85] The discrepancy may be attributed to the rotatable bonds between the thiophene rings of α-6T in solution. Bond rotation effectively breaks the π-conjugation and divides the molecule into smaller conjugated segments, increasing the energy gap between occupied and virtual orbitals and consequently the excitation energy observed in experiments,[76,77] as shown in the ESI.† Becker *et al.* experimentally observed a significant red shift of the absorption maxima of oligothiophenes upon cooling from 298 to 77 K. They ascribed the temperature dependence to molecular planarity.[77] At low temperatures, there is greater average planarity among thiophene rings, which is closer to the optimal planar geometry in the excited state. Therefore, the vertical excitation populates a lower vibronic level of the excited state. Notably, the experimental absorption maximum in Fig. 2 was measured at 77 K. Upon decreasing the temperature further, towards 0 K, the experimental observation may further decrease, becoming closer to the calculated value. Overall, based on the results presented here, and considering the very small systematic redshift of the B3LYP functional and the negligible solvent effect, we are confident that the TDDFT@B3LYP method is sufficiently accurate for the comparative assessment of prospective TTA chromophores.

3 Results and discussion

Fig. 3 shows the calculated $E^{loss}_{TTA,T}$ as a function of $E^{loss}_{TTA,S}$ for small graphene flakes consisting of 3, 4, or 5 conjugated aromatic rings (**16** to **29**, arranged by molecular size), benzo[*a*]pentacene (BP, **30**), and four experimentally observed TTA emitters. Experimentally observed emitters are indicated

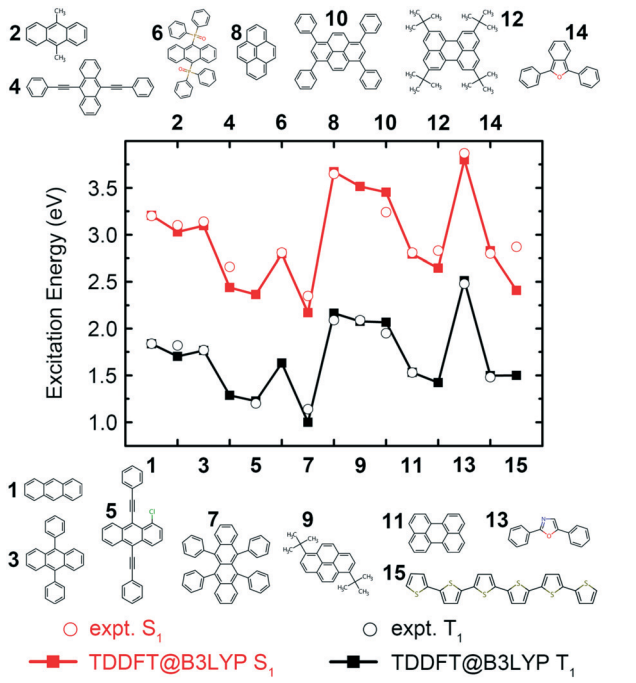

Fig. 2 The lowest singlet (red) and triplet (black) excitation energies of 15 experimentally observed TTA emitters, calculated with TDDFT@B3LYP, compared to experimental values extracted from absorption spectra in solution.[17,20,33,57–78] Tabulated experimental values and the solvents used are reported in the ESI.†

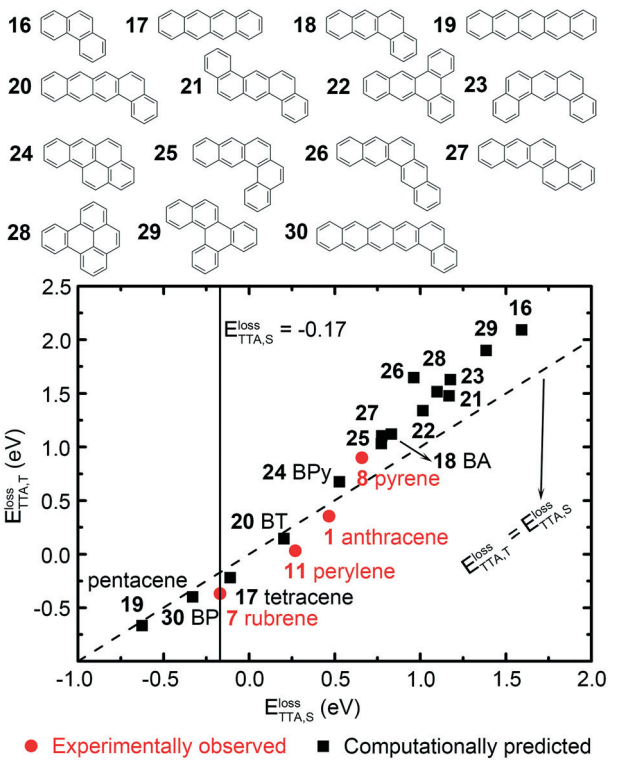

Fig. 3 The energy loss in the triplet pathway, $E^{loss}_{TTA,T}$, *vs.* the energy loss in the singlet pathway, $E^{loss}_{TTA,S}$, obtained from TDDFT@B3LYP calculations. Experimentally observed TTA emitters are indicated in red. The vertical line is $E^{loss}_{TTA,S}$ = −0.17 eV. The dashed line is $E^{loss}_{TTA,T} = E^{loss}_{TTA,S}$.

in red. In rubrene, the TTA singlet pathway is experimentally known to be approximately isoergic, $E_{TTA,S}^{loss} \approx 0$.[86] This is reproduced in TDDFT@B3LYP calculation with a small underestimation of 0.17 eV. Therefore, $E_{TTA,S}^{loss} = -0.17$ eV, indicated by a vertical line in Fig. 3, is considered as the lower bound for the singlet pathway to be open. Molecules with $E_{TTA,S}^{loss}$ greater than rubrene are candidate TTA emitters. Otherwise, they may be more likely to undergo SF. There is no upper bound for $E_{TTA,S}^{loss}$, however the conversion efficiency of solar energy decreases as the energy loss increases. $E_{TTA,T}^{loss} = E_{TTA,S}^{loss}$ is indicated by a dashed line in Fig. 3. Molecules below this line are preferred for TTA-UC because the main competing triplet pathway is energetically less favorable than the singlet pathway and therefore they are expected to have a higher QY. The $E_{TTA,T}^{loss}$ for rubrene obtained with TDDFT@B3LYP is −0.37 eV, slightly smaller than the experimental value of −0.074 eV observed in toluene.[86,87] This discrepancy may stem from the effects of temperature, solvent, and conformational flexibility in experiments, as well as the choice of approximation for the exchange–correlation functional in the calculations. Overall, the computational results are reliable, especially for qualitative trends among different molecules.

In Fig. 3, the singlet pathway of the experimentally observed emitters, anthracene, pyrene, and perylene, is exothermic due to a positive $E_{TTA,S}^{loss}$. Most of the small PAHs considered here have a $E_{TTA,S}^{loss}$ larger than rubrene and are thus candidate emitters. Pentacene, which is a well known SF material, and BP, have a smaller $E_{TTA,S}^{loss}$ than rubrene. The $E_{TTA,S}^{loss}$ of tetracene, a known SF chromophore, is very close to rubrene. This explains why TTA has also been observed for tetracene in solutions and solids.[88] In molecules, the S_1 state is usually dominated by the transition from the highest occupied molecular orbital (HOMO) to the lowest unoccupied molecular orbital (LUMO). Although the T_2 state may be dominated by other transitions, its excitation energy also depends largely on the gap between occupied and virtual orbitals, similarly to S_1. Consequently, $E_{TTA,T}^{loss}$ generally increases with $E_{TTA,S}^{loss}$ in Fig. 3. The triplet pathway is typically open together with the singlet pathway in emitters because the T_2 state is not likely to be much higher than S_1 in energy. The experimentally observed emitters rubrene, perylene, and anthracene stand out as having approximately the same energy loss in the singlet and triplet pathways. Pyrene and most of the other prospective TTA emitters studied here have a relatively high $E_{TTA,T}^{loss}$ and are therefore expected to have a lower QY. Finding a chromophore whose triplet pathway is energetically less favorable than its singlet pathway or ideally closed, is thus extremely challenging.

The TTA energetics have a strong dependence on the properties of chemical families and molecular size. For example, within the acene family, rubrene, which is a derivative of tetracene, may undergo SF or TTA in different states of matter and environments.[6,89–91] Pentacene and its derivatives are quintessential SF materials,[24,92–94] whereas anthracene and its derivatives are known TTA emitters.[6,9,15,95] This is because the $E_{TTA,S}^{loss}$ exhibits an inverse dependence on the length of the acene backbone.[14,24,96,97] As shown in Fig. 3, as the molecular length increases, the $E_{TTA,S}^{loss}$ decreases from a positive value for anthracene, to approximately zero for tetracene and rubrene, to a negative value for pentacene. This trend of TTA energetics as a function of molecular size is also found in benzo[*a*]anthracene (BA, **18**), BT, and BP in Fig. 3. Based on energetic criteria, we identify BP as a potential SF chromophore, possibly rivalling pentacene in terms of energy conversion efficiency, thanks to a smaller energy loss. Similar to BP, the $E_{TTA,S}^{loss}$ of BT and BA are also shifted to higher energy compared to tetracene and anthracene. BA has already been computationally studied as a prospective TTA emitter.[33,52] However, its $E_{TTA,S}^{loss}$ is larger than experimentally observed emitters. This means that even if it does undergo TTA, it is unlikely to be useful for practical applications, owing to a low conversion efficiency. Our energetics assessment shows that BT is a more promising candidate, thanks to a smaller energy loss in its singlet pathway, $E_{TTA,S}^{loss}$, and a smaller energy loss in the triplet pathway relative to the singlet pathway, $E_{TTA,T}^{loss} - E_{TTA,S}^{loss}$. The energetics of BT are very close to perylene, which is a well-known TTA emitter. We note that phenanthrene (**16**) has a similar molecular geometry to BA, BT, and BP, but has the largest energy losses in both singlet and triplet pathways. Despite the structural similarity, its electronic properties, such as the molecular orbitals, are significantly different from BA, BT, and BP, as shown in the ESI.† Another potential TTA emitter revealed in Fig. 3 is BPy. Its $E_{TTA,S}^{loss}$ and $E_{TTA,T}^{loss}$ are between those of anthracene and pyrene. Other chromophores considered here (**21** to **23** and **25** to **29**) are concentrated in the region of $0.77\ \text{eV} < E_{TTA,S}^{loss} < 1.39$ eV and $1.03\ \text{eV} < E_{TTA,T}^{loss} < 1.90$ eV, where the energy losses are too high, corresponding to a low solar energy conversion efficiency. Therefore, of the small PAHs in Fig. 3, BT and BPy are the most promising. Their energy release in the singlet and triplet pathways are comparable to those of experimentally observed emitters and superior to BA, which was previously proposed computationally.

The electronic and excitonic properties of anthracene, tetracene, pentacene, BA, BT, and BP are similar. Fig. 4 shows the density functional theory (DFT) energies of the HOMO–LUMO gaps. Visualizations of the HOMO and LUMO are also shown. The DFT@B3LYP HOMO–LUMO gap decreases from 3.57 eV in anthracene through 2.76 eV in tetracene to 2.19 eV in pentacene. The gap narrowing stems from the extended π-conjugation length of the frontier orbitals.[24,98,99] The benzene substitution on the terminals of BA, BT, and BP has a very limited effect on the spatial distribution and energies of frontier orbitals. The HOMO and LUMO are slightly extended to the additional benzene ring, leaving the charge distribution on the acene segment unchanged. The HOMO–LUMO gap decreases from 3.74 eV in BA through 2.93 eV in BT, to 2.34 eV in BP. Compared to the unsubstituted acenes, the HOMO–LUMO gaps of BA, BT, and BP increase by less than 0.20 eV. This small energy difference leads to slightly larger excitation energies of BA, BT, and BP than anthracene,

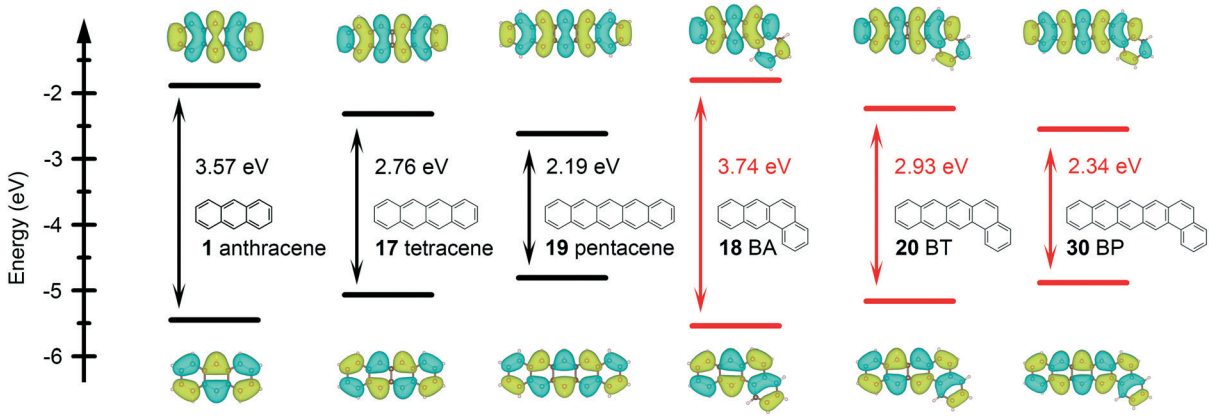

Fig. 4 The HOMO–LUMO gaps, obtained with DFT@B3LYP, and visualizations of frontier orbitals of anthracene, tetracene, pentacene, BA, BT, and BP.

tetracene, and pentacene in Fig. 5 and further contributes to the shift of $E_{TTA,S}^{loss}$ and $E_{TTA,T}^{loss}$ to higher energies in Fig. 3. A computational study has found that BT exhibits a high charge transfer rate and is more stable than its acene analogue, pentacene, benefiting device applications.[100] As shown in Fig. 5, the trends in S_1, T_1, and T_2 track the change in the ground state energy gap between occupied and virtual orbitals. One outlier is the T_2 energy of BA, which is 0.29 eV lower than S_1, owing to different transitions involved as shown in the ESI.† This leads to the triplet pathway being more energetically favorable than the singlet pathway for BA, which is detrimental to TTA. In comparison, the prospective TTA emitter, BT, is superior to BA thanks to very close S_1 and T_2 excitation energies.

The excitation energies of chromophores may be modulated by chemical functionalization.[19,24,101] We turn to investigating the effect of chemical modification on the TTA energetics of BT and BPy. Three side-groups of methyl (Me), *tert*-butyl (*t*Bu), and phenyl (Ph) are considered. Substituted BT and BPy, denoted as BT-2R and BPy-3R (R = Me, *t*Bu, or Ph), are illustrated in Fig. 6(a). Fig. 6(b) shows the $E_{TTA,S}^{loss}$ and $E_{TTA,T}^{loss}$ for BT, BPy, their derivatives, compared to four experimentally observed emitters. The addition of side-groups decreases the energy losses in the singlet and triplet pathways for BT and BPy. Specifically, the $E_{TTA,S}^{loss}$ of BT decreases slightly in BT-2Ph and BT-2Me and by more than 0.40 eV in BT-2*t*Bu, to the extent that BT-2*t*Bu is

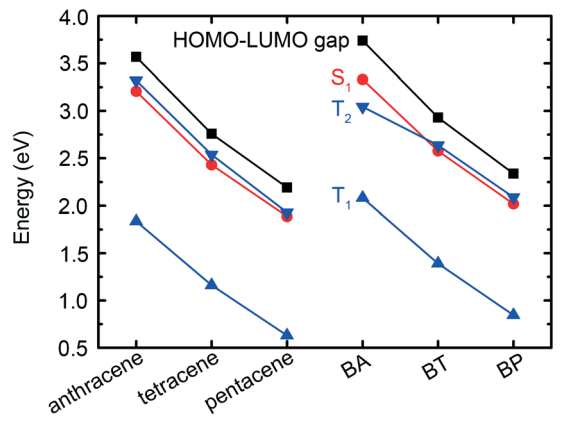

Fig. 5 The HOMO–LUMO gaps and S_1, T_1, and T_2 excitation energies of anthracene, tetracene, pentacene, BA, BT, and BP.

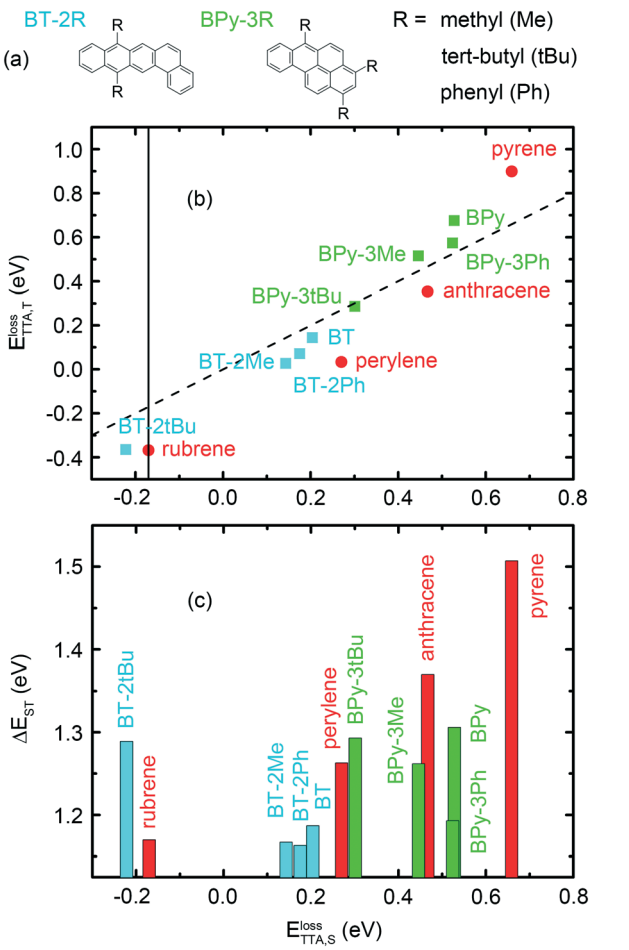

Fig. 6 (a) Molecular geometries of BT and BPy derivatives. (b) The energy loss in the triplet pathway, $E_{TTA,T}^{loss}$, *vs.* the energy loss in the singlet pathway, $E_{TTA,S}^{loss}$, obtained from TDDFT@B3LYP calculations. (c) The energy difference between the lowest singlet and triplet excitation states, ΔE_{ST}, *vs.* the energy loss in the singlet pathway, $E_{TTA,S}^{loss}$. Experimentally observed emitters are indicated in red.

located to the left of rubrene, in the SF range. The $E^{loss}_{TTA,S}$ of BPy also decreases in BPy-3Ph, BPy-3Me, and BPy-3*t*Bu, but they still have a larger $E^{loss}_{TTA,S}$ than BT and its derivatives. For both the BT and BPy series, the *t*Bu group exhibits a stronger ability of reducing energy losses than Me and Ph groups. This effect of *t*Bu substitution is also observed in known TTA emitters. For example, the *t*Bu substituted perylene, 2,5,8,11-tetra-*tert*-butylperylene, exhibits a smaller $E^{loss}_{TTA,S}$ and $E^{loss}_{TTA,T}$ than perylene.[14] The $E^{loss}_{TTA,T} - E^{loss}_{TTA,S}$ for BT, BPy, and their derivatives is larger than rubrene, perylene, and anthracene, but smaller than pyrene. Although the energy losses in singlet and triplet pathways of BT and BPy may be effectively reduced to improve the energy conversion efficiency by chemical modification, decreasing $E^{loss}_{TTA,T} - E^{loss}_{TTA,S}$ is difficult. Interestingly, the Ph substitution reduces $E^{loss}_{TTA,T}$ for BPy by more than 0.10 eV with a negligible change of $E^{loss}_{TTA,S}$. For a TTA emitter that exhibits a very small positive $E^{loss}_{TTA,S}$ and $E^{loss}_{TTA,T}$, chemical modification may energetically close the triplet pathway, leaving the singlet pathway open.

The minimization of $E^{loss}_{TTA,S}$ and maximization of ΔE_{ST} may be achieved simultaneously, as shown in Fig. 1(c). Fig. 6(c) shows the ΔE_{ST} of BT, BPy, and their derivatives, compared to four experimentally observed emitters, as a function of $E^{loss}_{TTA,S}$. Although in general $E^{loss}_{TTA,S}$ and ΔE_{ST} are independent of each other, for the four experimentally observed emitters shown here, molecules with a smaller $E^{loss}_{TTA,S}$, happen to have a smaller ΔE_{ST}. In this respect, BT and BPy derivatives functionalized with *t*Bu are better emitters. The *t*Bu substitution reduces the energy loss of the singlet pathway for BPy by 0.23 eV without a change of ΔE_{ST}. The BPy-3*t*Bu becomes comparable to perylene in Fig. 6(c). For BT, the *t*Bu substitution decreases $E^{loss}_{TTA,S}$ and increases ΔE_{ST}. However, BT-2*t*Bu has a slightly smaller $E^{loss}_{TTA,S}$ than rubrene and may therefore undergo SF, rather than TTA.

We note that the excitation energies calculated here are for isolated molecules. The chemical environment, *i.e.*, whether the molecule is in a crystalline or amorphous solid or in solution, also affects the excitation energies. For example, TTA has been observed for rubrene in solutions,[6] whereas the reverse process of SF has been reported in rubrene crystals[89] and amorphous films.[90] Neutral (optical) excitation energies are the difference between the fundamental gap and the exciton binding energy. The fundamental energy gap decreases from isolated molecules to the solid state, owing to the polarization energy of the dielectric screening and is further narrowed by the band dispersion resulting from electronic coupling between the frontier orbitals of neighboring molecules.[24,102] The exciton binding energy also differs between isolated molecules and solids due to the different spatial distributions of exciton wavefunctions. For example, the excited states of rubrene are valence states for a molecule in the gas phase, but they may be extended over several neighboring molecules in crystals, exhibiting a large percentage of CT character.[25,103] Therefore, once a promising prospective TTA candidate has been identified based on the energetics of an isolated molecule, further evaluation of the excitation energies should be performed for known or predicted crystal structures and/or for potential solvents that could be used in practice. The three energetic criteria suggested here are necessary but not sufficient conditions for TTA to occur with a high QY. Additional considerations may be necessary for practical applications. For example, the chemical environment in the solid state or in solution should be conducive to TTET from sensitizers to emitters. The emitters are additionally required to exhibit weak ISC from S_1 to T_1 and strong photoluminescence, such that upconverted singlet excitons mainly decay radiatively.

4 Conclusion

Experimentally observed TTA emitters are rare and their device applications are limited by low QY and small anti-Stokes shifts. We have analyzed the effect of the molecular excitation energies of TTA emitters on the efficiency of TTA-UC. First, the energy loss in the singlet pathway $E^{loss}_{TTA,S}$ determines whether a molecule is a putative TTA emitter or SF chromophore. A positive $E^{loss}_{TTA,S}$ is necessary for thermodynamically driving TTA, but a large energy loss decreases the solar energy conversion efficiency. Second, the TTA QY is typically low due to the presence of the competing triplet pathway. Ideally, if the energy loss in the triplet pathway $E^{loss}_{TTA,T}$ is negative, *i.e.*, if T_2 is larger than $2T_1$, the triplet pathway is energetically forbidden. Molecules that meet this requirement are extremely rare, therefore we search for molecules whose $E^{loss}_{TTA,T}$ is smaller than $E^{loss}_{TTA,S}$, such that the triplet pathway is less favorable than the singlet pathway. Third, in order to harvest as much as possible of the solar spectrum, the anti-Stokes shift should be maximized. The anti-Stokes shift cannot exceed the energy difference between the lowest singlet and triplet states ΔE_{ST}, which should thus be maximized. These criteria establish the energetic requirements for TTA to occur as efficiently as possible.

We have performed TDDFT@B3LYP calculations for the excitation energies of small PAHs. Most of the chromophores studied here have an exothermic TTA singlet pathway. However, for most of these, $E^{loss}_{TTA,T}$ is larger than $E^{loss}_{TTA,S}$, leading to an open competing triplet pathway and hence a low TTA QY. Discovering a TTA emitter, whose singlet pathway is energetically much more favorable than its triplet pathway remains a challenge. The $E^{loss}_{TTA,S}$ and $E^{loss}_{TTA,T}$ of BT and BPy are close to each other and comparable to those of experimentally observed emitters. Therefore, BT and BPy are identified as prospective emitters. Their energy losses in singlet and triplet pathways may be further tuned by chemical modification. In particular, the *t*Bu side-group tends to significantly decrease the energy losses in the singlet and triplet pathways and simultaneously increase the anti-Stokes shifts. The chemical compound space is still largely unexplored. Computer simulations may help the discovery and design of additional prospective TTA chromophores based on the energetic criteria proposed here. This would ultimately help improve solar energy conversion efficiency by harvesting more of the lower energy range of the solar spectrum *via* upconversion.

Conflicts of interest

There are no conflicts to declare.

Acknowledgements

The authors thank the Natural Science Foundation of Shandong Province, China (Grant No. ZR2020QB073) and the Fundamental Research Funds of Shandong University. Work at CMU was supported by the National Science Foundation (NSF) Division of Materials Research through grant DMR-2021803. This research used resources of the Argonne Leadership Computing Facility (ALCF), which is a DOE Office of Science User Facility supported under Contract DE-AC02-06CH11357 and of the National Energy Research Scientific Computing Center (NERSC), a DOE Office of Science User Facility supported by the Office of Science of the U.S. Department of Energy, under Contract DE-AC02-05CH11231.

Notes and references

1 W. Shockley and H. J. Queisser, *J. Appl. Phys.*, 1961, **32**, 510–519.
2 T. F. Schulze and T. W. Schmidt, *Energy Environ. Sci.*, 2015, **8**, 103–125.
3 P. Zhang, L. Liang and X. Liu, *J. Mater. Chem. C*, 2021, **9**, 16110–16131.
4 Y. C. Simon and C. Weder, *J. Mater. Chem.*, 2012, **22**, 20817–20830.
5 N. Yanai and N. Kimizuka, *Chem. Commun.*, 2016, **52**, 5354–5370.
6 T. N. Singh-Rachford and F. N. Castellano, *Coord. Chem. Rev.*, 2010, **254**, 2560–2573.
7 T. W. Schmidt and F. N. Castellano, *J. Phys. Chem. Lett.*, 2014, **5**, 4062–4072.
8 J. C. Goldschmidt and S. Fischer, *Adv. Opt. Mater.*, 2015, **3**, 510–535.
9 W. Ahmad, J. Wang, H. Li, Q. Ouyang, W. Wu and Q. Chen, *Coord. Chem. Rev.*, 2021, **439**, 213944.
10 J. Zhao, W. Wu, J. Sun and S. Guo, *Chem. Soc. Rev.*, 2013, **42**, 5323–5351.
11 D. L. Dexter, *J. Chem. Phys.*, 1953, **21**, 836–850.
12 X. Leng, F. Jin, M. Wei, H. Ma, J. Feng and Y. Ma, *J. Chem. Phys.*, 2019, **150**, 164107.
13 X. Guo, Y. Liu, Q. Chen, D. Zhao and Y. Ma, *Adv. Opt. Mater.*, 2018, **6**, 1700981.
14 X. Wang, R. Tom, X. Liu, D. N. Congreve and N. Marom, *J. Mater. Chem. C*, 2020, **8**, 10816–10824.
15 V. Gray, D. Dzebo, M. Abrahamsson, B. Albinsson and K. Moth-Poulsen, *Phys. Chem. Chem. Phys.*, 2014, **16**, 10345–10352.
16 Y. Y. Cheng, T. Khoury, R. G. Clady, M. J. Tayebjee, N. Ekins-Daukes, M. J. Crossley and T. W. Schmidt, *Phys. Chem. Chem. Phys.*, 2010, **12**, 66–71.
17 J. Zhao, S. Ji and H. Guo, *RSC Adv.*, 2011, **1**, 937–950.
18 V. Abraham and N. J. Mayhall, *J. Phys. Chem. Lett.*, 2021, **12**, 10505–10514.
19 J. L. Weber, E. M. Churchill, S. Jockusch, E. J. Arthur, A. B. Pun, S. Zhang, R. A. Friesner, L. M. Campos, D. R. Reichman and J. Shee, *Chem. Sci.*, 2021, **12**, 1068–1079.
20 V. Gray, A. Dreos, P. Erhart, B. Albinsson, K. Moth-Poulsen and M. Abrahamsson, *Phys. Chem. Chem. Phys.*, 2017, **19**, 10931–10939.
21 S. Hoseinkhani, R. Tubino, F. Meinardi and A. Monguzzi, *Phys. Chem. Chem. Phys.*, 2015, **17**, 4020–4024.
22 K. J. Fallon, E. M. Churchill, S. N. Sanders, J. Shee, J. L. Weber, R. Meir, S. Jockusch, D. R. Reichman, M. Y. Sfeir, D. N. Congreve and L. M. Campos, *J. Am. Chem. Soc.*, 2020, **142**, 19917–19925.
23 A. Yakubovich, A. Odinokov, S. Nikolenko, Y. Jung and H. Choi, *Front. Chem.*, 2021, **9**, 1128.
24 X. Wang, X. Liu, R. Tom, C. Cook, B. Schatschneider and N. Marom, *J. Phys. Chem. C*, 2019, **123**, 5890–5899.
25 X. Liu, R. Tom, X. Wang, C. Cook, B. Schatschneider and N. Marom, *J. Phys.: Condens. Matter*, 2020, **32**, 184001.
26 Y. Wei, Y. Li, M. Zheng, X. Zhou, Y. Zou and C. Yang, *Adv. Opt. Mater.*, 2020, **8**, 1902157.
27 C. Fan, L. Wei, T. Niu, M. Rao, G. Cheng, J. J. Chruma, W. Wu and C. Yang, *J. Am. Chem. Soc.*, 2019, **141**, 15070–15077.
28 N. Yanai, M. Kozue, S. Amemori, R. Kabe, C. Adachi and N. Kimizuka, *J. Mater. Chem. C*, 2016, **4**, 6447–6451.
29 W. Chen, F. Song, S. Tang, G. Hong, Y. Wu and X. Peng, *Chem. Commun.*, 2019, **55**, 4375–4378.
30 J. Peng, X. Guo, X. Jiang, D. Zhao and Y. Ma, *Chem. Sci.*, 2016, **7**, 1233–1237.
31 A. M. Polgar and Z. M. Hudson, *Chem. Commun.*, 2021, **57**, 10675–10688.
32 T. J. B. Zähringer, M.-S. Bertrams and C. Kerzig, *J. Mater. Chem. C*, 2022, **10**, 4568–4573.
33 A. S. Gertsen, M. Koerstz and K. V. Mikkelsen, *Phys. Chem. Chem. Phys.*, 2018, **20**, 12182–12192.
34 E. Runge and E. K. U. Gross, *Phys. Rev. Lett.*, 1984, **52**, 997–1000.
35 W. Liu and Y. Xiao, *Chem. Soc. Rev.*, 2018, **47**, 4481–4509.
36 F. Neese, *WIREs Comput. Mol. Sci.*, 2012, **2**, 73–78.
37 S. Grimme, S. Ehrlich and L. Goerigk, *J. Comput. Chem.*, 2011, **32**, 1456–1465.
38 P. J. Stephens, F. J. Devlin, C. F. Chabalowski and M. J. Frisch, *J. Phys. Chem.*, 1994, **98**, 11623–11627.
39 A. Dreuw and M. Head-Gordon, *Chem. Rev.*, 2005, **105**, 4009–4037.
40 A. Dreuw and M. Head-Gordon, *J. Am. Chem. Soc.*, 2004, **126**, 4007–4016.
41 O. Gritsenko and E. J. Baerends, *J. Chem. Phys.*, 2004, **121**, 655–660.
42 S. Kümmel, *Adv. Energy Mater.*, 2017, **7**, 1700440.
43 S. Grimme, *J. Chem. Phys.*, 2006, **124**, 034108.
44 A. Karton, A. Tarnopolsky, J.-F. Lamère, G. C. Schatz and J. M. L. Martin, *J. Phys. Chem. A*, 2008, **112**, 12868–12886.

45 D. Mester and M. Kallay, *J. Chem. Theory Comput.*, 2022, **18**, 1646–1662.
46 F. Della Sala and A. Gorling, *Int. J. Quantum Chem.*, 2003, **91**, 131–138.
47 R. J. Cave, F. Zhang, N. T. Maitra and K. Burke, *Chem. Phys. Lett.*, 2004, **389**, 39–42.
48 N. T. Maitra, F. Zhang, R. J. Cave and K. Burke, *J. Chem. Phys.*, 2004, **120**, 5932–5937.
49 D. Jacquemin, V. Wathelet, E. A. Perpète and C. Adamo, *J. Chem. Theory Comput.*, 2009, **5**, 2420–2435.
50 A. D. Laurent and D. Jacquemin, *Int. J. Quantum Chem.*, 2013, **113**, 2019–2039.
51 S. S. Leang, F. Zahariev and M. S. Gordon, *J. Chem. Phys.*, 2012, **136**, 104101.
52 M. Alipour and Z. Safari, *Phys. Chem. Chem. Phys.*, 2019, **21**, 17126–17141.
53 T. Yanai, D. P. Tew and N. C. Handy, *Chem. Phys. Lett.*, 2004, **393**, 51–57.
54 C. S. Garoufalis and A. D. Zdetsis, *Phys. Chem. Chem. Phys.*, 2006, **8**, 808–813.
55 M. Zhao, F. Yang, Y. Xue, D. Xiao and Y. Guo, *ChemPhysChem*, 2014, **15**, 950–957.
56 Y. Tawada, T. Tsuneda, S. Yanagisawa, T. Yanai and K. Hirao, *J. Chem. Phys.*, 2004, **120**, 8425–8433.
57 J. Brinen and J. Koren, *Chem. Phys. Lett.*, 1968, **2**, 671–672.
58 H. Klevens and J. Platt, *J. Chem. Phys.*, 1949, **17**, 470–481.
59 C. Quarti, D. Fazzi and M. Del Zoppo, *Phys. Chem. Chem. Phys.*, 2011, **13**, 18615–18625.
60 T. N. Singh-Rachford, R. R. Islangulov and F. N. Castellano, *J. Phys. Chem. A*, 2008, **112**, 3906–3910.
61 R. R. Islangulov, J. Lott, C. Weder and F. N. Castellano, *J. Am. Chem. Soc.*, 2007, **129**, 12652–12653.
62 T. Miteva, V. Yakutkin, G. Nelles and S. Baluschev, *New J. Phys.*, 2008, **10**, 103002.
63 Y. Che, W. Yang, G. Tang, F. Dumoulin, J. Zhao, L. Liu and Ü. İşci, *J. Mater. Chem. C*, 2018, **6**, 5785–5793.
64 R. Tao, J. Zhao, F. Zhong, C. Zhang, W. Yang and K. Xu, *Chem. Commun.*, 2015, **51**, 12403–12406.
65 W. Herkstroeter and P. Merkel, *J. Photochem.*, 1981, **16**, 331–341.
66 A. Nakajima, *Bull. Chem. Soc. Jpn.*, 1971, **44**, 3272–3277.
67 D. Fornasiero and F. Grieser, *J. Chem. Soc., Faraday Trans.*, 1990, **86**, 2955–2960.
68 H. Bettermann, *Spectrochim. Acta, Part A*, 1994, **50**, 1073–1079.
69 C. Rulliere, E. Colson and P. Roberge, *Can. J. Chem.*, 1975, **53**, 3269–3275.
70 L. Latterini, G. Massaro, M. Penconi, P. Gentili, C. Roscini and F. Ortica, *Dalton Trans.*, 2018, **47**, 8557–8565.
71 Y. Sasaki, S. Amemori, H. Kouno, N. Yanai and N. Kimizuka, *J. Mater. Chem. C*, 2017, **5**, 5063–5067.
72 B. D. Ravetz, A. B. Pun, E. M. Churchill, D. N. Congreve, T. Rovis and L. M. Campos, *Nature*, 2019, **565**, 343.
73 F. S. Dainton, T. Morrow, G. Salmon and G. Thompson, *Proc. R. Soc. London, Ser. A*, 1972, **328**, 457–479.
74 T. Takahashi, K. Kikuchi and H. Kokubun, *J. Photochem.*, 1980, **14**, 67–76.
75 M. B. Smith and J. Michl, *Chem. Rev.*, 2010, **110**, 6891–6936.
76 A. Yassar, G. Horowitz, P. Valat, V. Wintgens, M. Hmyene, F. Deloffre, P. Srivastava, P. Lang and F. Garnier, *J. Phys. Chem.*, 1995, **99**, 9155–9159.
77 R. S. Becker, J. Seixas de Melo, A. L. Macanita and F. Elisei, *J. Phys. Chem.*, 1996, **100**, 18683–18695.
78 W. Zhao and F. N. Castellano, *J. Phys. Chem. A*, 2006, **110**, 11440–11445.
79 C. Aleman, J. Torras and J. Casanovas, *Chem. Phys. Lett.*, 2011, **511**, 283–287.
80 H. Sun and J. Autschbach, *J. Chem. Theory Comput.*, 2014, **10**, 1035–1047.
81 J. Seixas de Melo, F. Elisei, C. Gartner, G. G. Aloisi and R. S. Becker, *J. Phys. Chem. A*, 2000, **104**, 6907–6911.
82 M. S. Hybertsen and S. G. Louie, *Phys. Rev. B: Condens. Matter Mater. Phys.*, 1986, **34**, 5390.
83 M. Rohlfing and S. G. Louie, *Phys. Rev. B: Condens. Matter Mater. Phys.*, 2000, **62**, 4927.
84 N. Marom, *J. Phys.: Condens. Matter*, 2017, **29**, 103003.
85 S. Sharifzadeh, *J. Phys.: Condens. Matter*, 2018, **30**, 153002.
86 Y. Y. Cheng, B. Fückel, T. Khoury, R. G. Clady, M. J. Tayebjee, N. Ekins-Daukes, M. J. Crossley and T. W. Schmidt, *J. Phys. Chem. Lett.*, 2010, **1**, 1795–1799.
87 F. Lewitzka and H.-G. Löhmannsröben, *Z. Phys. Chem.*, 1986, **150**, 69–86.
88 H. Tachikawa and A. J. Bard, *Chem. Phys. Lett.*, 1973, **19**, 287–289.
89 L. Ma, K. Zhang, C. Kloc, H. Sun, M. E. Michel-Beyerle and G. G. Gurzadyan, *Phys. Chem. Chem. Phys.*, 2012, **14**, 8307–8312.
90 V. Jankus, E. W. Snedden, D. W. Bright, E. Arac, D. Dai and A. P. Monkman, *Phys. Rev. B: Condens. Matter Mater. Phys.*, 2013, **87**, 224202.
91 E. Radiunas, M. Dapkevicius, L. Naimovicius, P. Baronas, S. Raisys, S. Jursenas, A. Jozeliunaite, T. Javorskis, U. Sinkeviciute, E. Orentas and K. Kazlauskas, *J. Mater. Chem. C*, 2021, **9**, 4359–4366.
92 P. M. Zimmerman, Z. Zhang and C. B. Musgrave, *Nat. Chem.*, 2010, **2**, 648–652.
93 B. J. Walker, A. J. Musser, D. Beljonne and R. H. Friend, *Nat. Chem.*, 2013, **5**, 1019–1024.
94 S. Sharifzadeh, C. Y. Wong, H. Wu, B. L. Cotts, L. Kronik, N. S. Ginsberg and J. B. Neaton, *Adv. Funct. Mater.*, 2015, **25**, 2038–2046.
95 C. E. Elgar, H. Y. Otaif, X. Zhang, J. Zhao, P. N. Horton, S. J. Coles, J. M. Beames and S. J. A. Pope, *Chem. – Eur. J.*, 2021, **27**, 3427–3439.
96 T. Rangel, K. Berland, S. Sharifzadeh, F. Brown-Altvater, K. Lee, P. Hyldgaard, L. Kronik and J. B. Neaton, *Phys. Rev. B*, 2016, **93**, 115206.
97 Y. Y. Pan, J. Huang, Z. M. Wang, D. W. Yu, B. Yang and Y. G. Ma, *RSC Adv.*, 2017, **7**, 26697–26703.
98 E. Fabiano, F. D. Sala, R. Cingolani, M. Weimer and A. Görling, *J. Phys. Chem. A*, 2005, **109**, 3078–3085.

99 K. Hummer and C. Ambrosch-Draxl, *Phys. Rev. B: Condens. Matter Mater. Phys.*, 2005, **72**, 205205.
100 L. Jones and L. Lin, *J. Phys. Chem. A*, 2017, **121**, 2804–2813.
101 E. Cho, V. Coropceanu and J.-L. Bredas, *J. Mater. Chem. C*, 2021, **9**, 10794–10801.
102 S. Monaco, R. P. Baer, R. P. Giernacky, M. E. Villalba, T. M. Garcia, C. Mora-Perez, S. E. Brady, K. D. Erlitz, C. Kunkel, S. R. Jezowski, H. Oberhofer, C. Lange and B. Schatschneider, *Comput. Mater. Sci.*, 2021, **197**, 110510.
103 X. Wang, T. Garcia, S. Monaco, B. Schatschneider and N. Marom, *CrystEngComm*, 2016, **18**, 7353–7362.